

## Article

# Electrospun Poly(methyl methacrylate)/TiO<sub>2</sub> Composites for Photocatalytic Water Treatment

Olya Stoilova <sup>\*</sup>, Nevena Manolova  and Iliya Rashkov 

Laboratory of Bioactive Polymers, Institute of Polymers, Bulgarian Academy of Sciences, Akad. G. Bonchev St., bl. 103A, 1113 Sofia, Bulgaria; manolova@polymer.bas.bg (N.M.); rashkov@polymer.bas.bg (I.R.)

\* Correspondence: stoilova@polymer.bas.bg

**Abstract:** Electrospinning was successfully used for the one-step fabrication of poly(methyl methacrylate) (PMMA) fibers loaded with an inorganic photocatalyst—titanium oxide (TiO<sub>2</sub>). By tuning the PMMA/TiO<sub>2</sub> ratio and the electrospinning conditions (applied voltage, needle tip-to-collector distance, and flow rates), PMMA/TiO<sub>2</sub> composites with selected organic/inorganic ratios, tailored designs, and targeted properties were obtained. The morphology of the electrospun composites was affected by the amount of TiO<sub>2</sub> incorporated into the PMMA fibers. In addition, the inorganic photocatalyst had an impact on the wettability, thermal stability, and optical properties of the electrospun composites. In particular, the surface wettability of the composites was strongly influenced by UV light irradiation and from hydrophobic became superhydrophilic. Moreover, PMMA/TiO<sub>2</sub> composites had enhanced tensile strength in comparison with those of bare PMMA mats. The electrospun PMMA/TiO<sub>2</sub> composites showed excellent photocatalytic efficiency against the model organic pollutant—methylene blue—which is very promising for the future development of membranes that are highly efficacious for photocatalytic water treatment.



**Citation:** Stoilova, O.; Manolova, N.; Rashkov, I. Electrospun Poly(methyl methacrylate)/TiO<sub>2</sub> Composites for Photocatalytic Water Treatment. *Polymers* **2021**, *13*, 3923. <https://doi.org/10.3390/polym13223923>

Academic Editor: Andreea-Teodora Iacob

Received: 25 October 2021

Accepted: 9 November 2021

Published: 13 November 2021

**Publisher's Note:** MDPI stays neutral with regard to jurisdictional claims in published maps and institutional affiliations.



**Copyright:** © 2021 by the authors. Licensee MDPI, Basel, Switzerland. This article is an open access article distributed under the terms and conditions of the Creative Commons Attribution (CC BY) license (<https://creativecommons.org/licenses/by/4.0/>).

**Keywords:** electrospinning; poly(methyl methacrylate); TiO<sub>2</sub>; UV-induced wettability; mechanical properties; photocatalysis

## 1. Introduction

The creation of cost-effective and advanced materials for water treatment is an ongoing challenge. Among the various new materials that have been created, electrospun membranes are considered to be the most versatile candidates for the effective treatment of water, filtration, and separation because of their high surface area, high porosity, and light weight [1,2]. In order to improve the applicability and performance of electrospun membranes for use in water treatment, metal oxide nanoparticles have been incorporated into membranes [2,3]. Thus, the key challenge in water treatment is to prepare appropriate electrospun composites with a high efficiency and low environmental impact.

Currently, great attention is being paid to photocatalysis, which is one of the most effective and ecofriendly techniques for the degradation of many organic pollutants [4–6]. In this regard, one of the most widely reported on and commonly used photocatalysts for the removal of organic pollutants is TiO<sub>2</sub> because of its ability to generate hydroxyl radicals (HO•) and superoxide radical anions (O<sup>2•-</sup>) upon UV light irradiation [7]. Furthermore, TiO<sub>2</sub> has found a wide range of applications due to its remarkable physical, electronic, dielectric, and optical properties, as well as its efficient photoactivity, high stability, low cost, and friendliness to the environment [7–9]. Various studies have revealed that poly(methyl methacrylate) (PMMA) is an appropriate host matrix for these photocatalysts because of its excellent transparency to light, good environmental inertness, chemical and thermal stability, and relatively low cost [10–12]. This is why PMMA-based composite films have played a major role in the preparation of light emitting diodes (LED), supercapacitors, optical lenses, sensors, catalysts, etc. Moreover, PMMA/TiO<sub>2</sub> nanocomposites have remained a

hot research topic for use in multifunctional applications, such as photocatalysts, protective coatings, and UV shields [13–17].

Electrospinning has emerged as an appropriate technique for preparing polymer composites loaded with inorganic particles. Although electrospun PMMA/TiO<sub>2</sub> composites have been recently reported on [18], to the best of our knowledge there has been no thorough study on the effect of the use of TiO<sub>2</sub> nanoparticles as fillers in uniform defect-free fibers on the properties of electrospun PMMA/TiO<sub>2</sub> composites. In the past few years, we have demonstrated the possibility of the fabrication of multifunctional hybrid materials by electrospinning [19–21]. Electrospun materials based on poly(3-hydroxybutyrate) and TiO<sub>2</sub> with tailored designs have displayed an excellent stability and been shown to be able to preserve their photocatalytic activity almost completely. In this context, in the present study commercially available TiO<sub>2</sub> nanoparticles were dispersed into PMMA solution in order to prepare composite PMMA fibers filled with TiO<sub>2</sub> in one step through electrospinning. By varying the TiO<sub>2</sub> content (5 and 10 wt. %) in the dispersions and the electrospinning conditions (applied voltage, needle tip-to-collector distance, and flow rates), optimal conditions were found for the formation of a stable Taylor cone and defect-free composite fibers. The morphology of the prepared electrospun composites was observed by scanning electron microscopy (SEM). The wettability, surface composition, and thermal and mechanical properties of the PMMA/TiO<sub>2</sub> composites were studied in detail by water contact angle measurements, X-ray photoelectron spectroscopy (XPS), thermogravimetric analyses (TGA), and tensile tests. The optical properties, photocatalytic activity when using methylene blue as a model organic pollutant, and reusability of the composites were evaluated with respect to targeted application.

## 2. Materials and Methods

### 2.1. Materials

Poly(methyl methacrylate) (PMMA, average molecular weight ~350,000 g/mol) and titanium (IV) oxide (TiO<sub>2</sub> nanopowder, 99.7% anatase) were purchased from Sigma Aldrich. *N,N*-dimethylformamide (DMF, p.a.) and methylene blue B (MB) were purchased from Merck. All reagents were of an analytical grade of purity and were used as received without further purification.

### 2.2. Electrospinning

Solutions of PMMA (15% *w/v*) in DMF were prepared by heating them at 50 °C using a reflux condenser. In order to obtain PMMA/5TiO<sub>2</sub> and PMMA/10TiO<sub>2</sub> composites, TiO<sub>2</sub> nanopowder (5 and 10 wt. % with respect to PMMA) was added to the PMMA solutions. The obtained dispersions were homogenized by sonication for 1 h in an ultrasonic bath (Bandelin Sonorex, Berlin, Germany, 160/640 W, 35 kHz).

The experimental electrospinning setup comprised a high-voltage DC power supply, rotating collector, needle for syringe (i.d. 0.6 mm × o.d. 0.9 mm), and syringe pump (NE-300 New Era Pump Systems, Inc., Farmingdale, NY, USA) for delivering the spinning dispersions. The electrospinning of the PMMA solution and PMMA/TiO<sub>2</sub> dispersions was performed at a 15 kV applied voltage with a needle tip-to-collector distance of 10 cm, a 2 mL/h flow rate, and a collector rotation speed of 1200 rpm. These optimal electrospinning conditions were identified through the testing of various combinations of processing parameters (applied voltage, flow rate, and needle tip-to-collector distance).

### 2.3. Characterization

The morphology of the electrospun PMMA/TiO<sub>2</sub> composites was observed using scanning electron microscopy (SEM). Specimens were vacuum-coated with gold in a Jeol JFC-1200 fine coater and analyzed using a Jeol JSM-5510 instrument (JEOL Co., Ltd., Tokyo, Japan). The Image J software was used to measure the average fiber diameter by measuring at least 15 fibers from each image. Transmission electron spectroscopy (TEM) observations of the PMMA/TiO<sub>2</sub> composites were carried out with a JEM-2100

instrument (JEOL Co., Ltd., Tokyo, Japan) equipped with selected area electron diffraction (SAED). Specimens were prepared by depositing on a copper grid. The surface chemical composition of the PMMA/TiO<sub>2</sub> composites was determined quantitatively by X-ray photoelectron spectroscopy (XPS). The measurements were carried out in the UHV chamber of an ESCALAB-MkII (VG Scientific, Waltham, MA, USA) spectrometer using Mg Ka excitation with a total instrumental resolution of ~1 eV. Energy calibration was performed, taking the C1s line at 285 eV as a reference. Surface atomic concentrations were evaluated using Scofield's ionization cross-sections with no corrections for  $\lambda$  (the mean free path of photoelectrons) and the analyzer transmission function. The experimental values for the element atomic percentages obtained from the XPS analysis were the average of three independent measurements. Water contact angles (WCA) were measured with a drop shape analyzer (DSA 20E, Krüss GmbH, Hamburg, Germany) at room temperature. Rectangular samples with a 15 mm width and 40 mm length were cut and fixed on glass slides (75 mm × 25 mm). Contact angles were measured before and after the UV light irradiation (UV lamp 400F/2, UVASPOT 400/T, Dr. Hönle AG, Gräfelfing, Germany) of the samples for 30 and 60 min. The distance from the UV lamp to the samples was 30 cm. A sessile drop of distilled water with a volume of 5  $\mu$ L controlled by a computer dosing system was deposited onto the samples. The contact angles were determined by commercial software (DSA 20E, Krüss GmbH) using the acquired images of the droplet. The data were averages taken from 10 measurements for each sample.

X-ray diffraction (XRD) analyses were performed using a D8 Bruker Advance diffractometer with filtered Cu K $\alpha$  radiation and a LynxEye detector at room temperature. XRD spectra were recorded in the  $2\theta$  range from 5.3° to 80° with a step size of 0.02° and counting time of 1 s/step. Phase identification was performed using the Diffracplus EVA using ICDD-PDF2 Database. Thermogravimetric analyses (TGA) were carried out on SetSys Evolution 2500 (Setaram, Caluire, France) at a heating rate of 10 °C/min and an argon flow of 30 mL/min. Emission spectra were recorded using a Cary Eclipse spectrofluorometer (Varian, Santa Clara, CA, USA). Rectangular specimens with a 10 mm width and 45 mm length were cut and their fluorescence spectra were recorded using quartz glass cells with 10 mm path length.

Tensile testing was performed at room temperature with a crosshead speed of 20 mm/min on a single column dynamometer INSTRON 3344 equipped with a 50 N load cell. Rectangular specimens with 20 mm widths and 60 mm lengths were cut in the collector rotation direction (0°). The thickness of each specimen was measured before the tensile test using a digital thickness gauge FD 50 (Käfer GmbH, Villingen-Schwenningen, Germany). The average values for the tensile strength ( $\sigma$ , MPa), elongation at break ( $\epsilon_B$ , %), and Young's modulus ( $E$ , MPa) were determined based on the regression of the linear part of the stress–strain curves from at least 10 tested specimens of each electrospun material.

#### 2.4. Photocatalytic Activity

The photocatalytic activity of the prepared electrospun materials was evaluated by the degradation of a model pollutant—methylene blue B (MB). A stock solution of MB ( $2 \times 10^{-5}$  mol/L) in distilled water was prepared and used for a photodegradation analysis. Electrospun samples with a size of 10 mm × 10 mm were cut and then immersed in 10 mL of the MB solution. In order to reach an adsorption–desorption equilibrium, samples were kept in the dark for 60 min and were then irradiated by UV light (UV lamp 400F/2, UVASPOT 400/T, Dr. Hönle AG, Ilmenau, Germany) for 3 h. The photocatalytic degradation of MB was monitored spectrophotometrically by recording the intensity decrease in the MB absorbance at 660 nm with the irradiation time. UV–vis spectra were recorded with a DU800 spectrophotometer (Beckman Coulter Inc., Brea, CA, USA).

The reusability potential of the composed materials was also studied. For that purpose, after the first 3 h run the electrospun samples were again reused in two subsequent cycles by immersing them in a fresh MB solution. This procedure was repeated three times for 3 h using the same electrospun samples. After each cycle, the materials were washed and

placed in fresh MB solution for the subsequent irradiation cycle. The photodegradation efficiency (PDE, %) was calculated from the following equation:

$$\text{PDE (\%)} = (C_0 - C_t)/C_0 \times 100,$$

where  $C_0$  and  $C_t$  are the initial MB concentration and the concentration at time  $t$ , respectively.

### 3. Results and Discussion

The focus of the present work was on the fabrication of PMMA fibers filled with significant amounts of  $\text{TiO}_2$  and studying the effect of the inorganic photocatalyst on the properties of the obtained electrospun PMMA/ $\text{TiO}_2$  composites with respect to their targeted application. Koysuren et al. reported the synthesis of  $\text{TiO}_2$  particles by the sol-gel process, their calcination and immobilization in PMMA fibers by electrospinning [18]. However, the results show that the appropriate conditions for obtaining defect-free fibers have not been found, which calls into question the results of the research conducted. Moreover, the crystal phase of the synthesized  $\text{TiO}_2$  particles was not studied, and the presented FTIR spectra proved the presence of an unreacted titanium isopropoxide precursor. In addition, the amount of calcinated  $\text{TiO}_2$  particles incorporated into the PMMA fibers was very low, this is why only 20% of the methylene blue was degraded after 180 min of UV irradiation.

In the present study, in order to avoid all of these disadvantages, commercially available  $\text{TiO}_2$  (anatase) nanopowder was used. Furthermore, preliminary experiments were performed and by varying the electrospinning conditions (applied voltage, needle tip-to-collector distance and flow rates), optimal terms for the formation of defect-free composite PMMA fibers were found. Moreover, besides the electrospinning conditions, the  $\text{TiO}_2$  content in the dispersions was also varied toward the fabrication of PMMA fibers filled with a significant amount of  $\text{TiO}_2$ . It was determined that the incorporation of the maximum amount of 10% of  $\text{TiO}_2$  nanopowder (with respect to PMMA) into the PMMA solution did not hamper the process of electrospinning and resulted in the preparation of continuous fibers. The effect of  $\text{TiO}_2$  on the properties of electrospun PMMA/ $\text{TiO}_2$  composites as a filler in PMMA fibers was studied in detail and the composition-structure-property dependence was determined.

#### 3.1. PMMA/ $\text{TiO}_2$ Composites Fabrication and Characterization

Preliminary experiments showed that the electrospinning (15 kV applied voltage, 10 cm needle tip-to-collector distance, and 2 mL/h flow rate) of PMMA spinning solution in DMF with a concentration of 15% *w/v* resulted in defect-free PMMA fibers. These conditions were found to be suitable and were used for the fabrication of defect-free composite PMMA fibers containing 5 and 10% of  $\text{TiO}_2$ .

The morphology of the fabricated PMMA/ $\text{TiO}_2$  composites was observed by SEM (Figure 1). The SEM micrographs clearly show that the selected concentrations and electrospinning conditions lead to the fabrication of cylindrical, uniform, and defect-free fibers with a certain fiber alignment in the direction of the collector rotation. Interestingly, the surface of the composite fibers was decorated with  $\text{TiO}_2$  (Figure 1C,E). Moreover, when the  $\text{TiO}_2$  concentration in the PMMA fibers was increased, the number of particles on the fiber surface increased (Figure 1E). This implies that part of the  $\text{TiO}_2$  loaded into the fibers aggregates during the electrospinning process and that the optimum photocatalyst concentration was reached, thus resulting in the particles being arranged not only in the PMMA fibers but also on their surface. The fiber diameter distribution is also presented in Figure 1. As expected, the  $\text{TiO}_2$  incorporation into the PMMA fibers resulted in a slight increase in their average fiber diameters—from  $1986 \pm 245$  nm for PMMA fibers (Figure 1B) to  $2079 \pm 257$  nm (Figure 1D) and  $2104 \pm 319$  nm (Figure 1F) for PMMA/5 $\text{TiO}_2$  and PMMA/10 $\text{TiO}_2$ , respectively. The SEM analyses clearly show that uniform and defect-free PMMA/ $\text{TiO}_2$  composite fibers were successfully fabricated in one step by electrospinning and that their morphologies depend on the  $\text{TiO}_2$  content in the PMMA fibers.

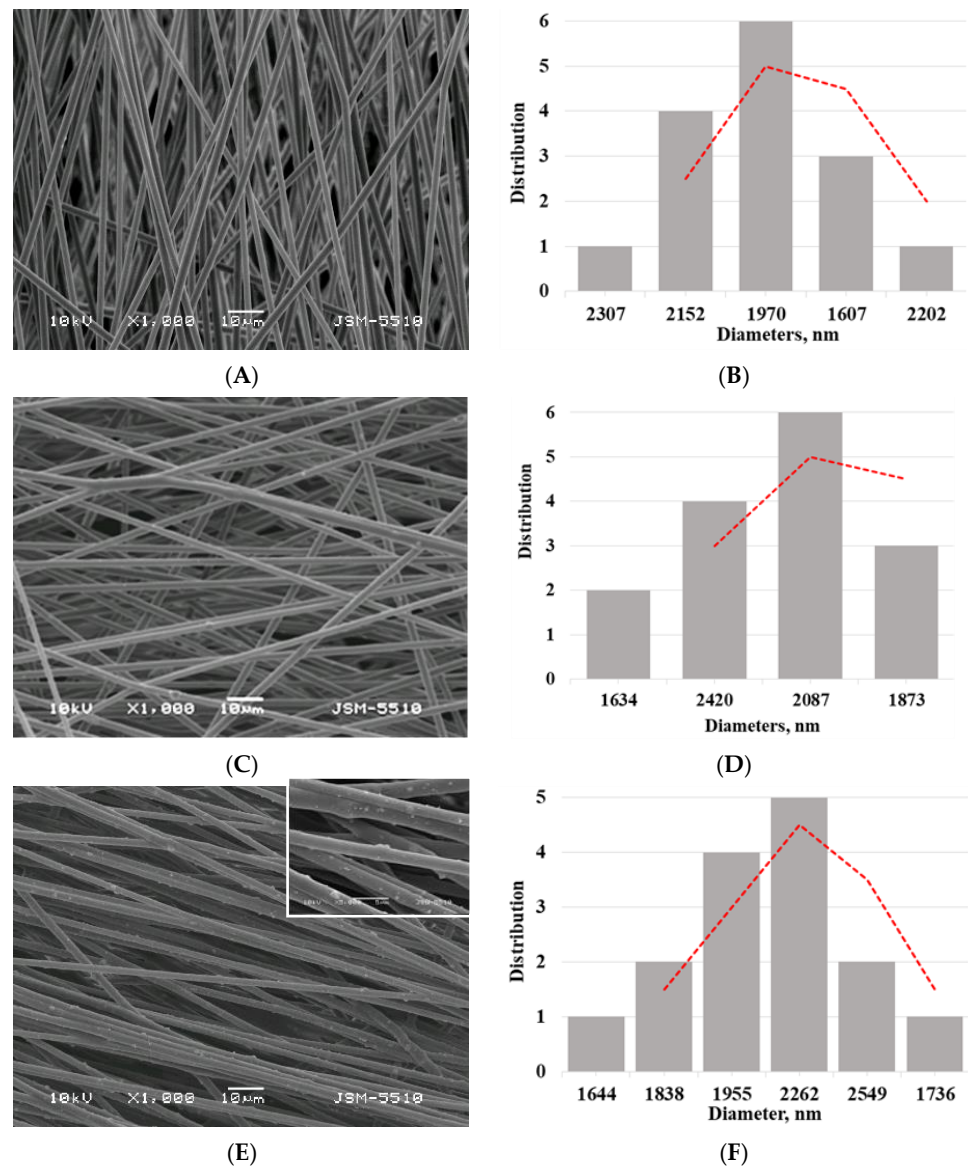


**Figure 1.** SEM micrographs and fibers diameter distribution of electrospun PMMA (A,B), PMMA/5TiO<sub>2</sub> (C,D), and PMMA/10TiO<sub>2</sub> (E,F) composites. Magnification  $\times 1000$ . Inset: magnification  $\times 5000$ .

The successful inclusion of the TiO<sub>2</sub> particles in the PMMA fibers was evidenced by TEM (Figure S1). As clearly seen, a part of TiO<sub>2</sub> formed agglomerates during the electrospinning process. In confirmation of the SEM observations, TEM analyses also clearly showed that the surface of the composite fibers was decorated with TiO<sub>2</sub>. In addition, the obtained SAED patterns showed strong diffraction spots evidencing the lattice spacing of the crystals, indexed to the anatase structure of TiO<sub>2</sub> (# 96-101-0943) with the lattice planes.

The surface chemical composition of the PMMA/TiO<sub>2</sub> fibers was evaluated by XPS analysis (Figure 2) and provided additional evidence regarding the titanium content on the fibers' surfaces. In the survey of the XPS spectra of PMMA/TiO<sub>2</sub> composite fibers, photoemission bands corresponding to C1s (285 eV), O1s (532.4 eV), and Ti2p (459 eV) were observed (Figure 2, left). As expected, in the Ti2p spectrum of PMMA/TiO<sub>2</sub> composites, one major peak was observed at 459 eV with a splitting of 5.7 eV for the Ti2p 3/2 and Ti2p 1/2 components of the doublet (Figure 2, right). The binding energy value is characteristic of titanium in its normal Ti<sup>4+</sup> oxidation state and is in good agreement with the value

reported in the literature [22]. By calculating the Ti/C atomic ratio, it was determined that the titanium content on the surface of PMMA/5TiO<sub>2</sub> (0.47%) was lower than that on the PMMA/10TiO<sub>2</sub> (0.82%) composites. Therefore, the XPS analysis further verified that the surface composition of the electrospun PMMA/TiO<sub>2</sub> composites was affected by the amount of TiO<sub>2</sub> incorporated in the PMMA fibers.

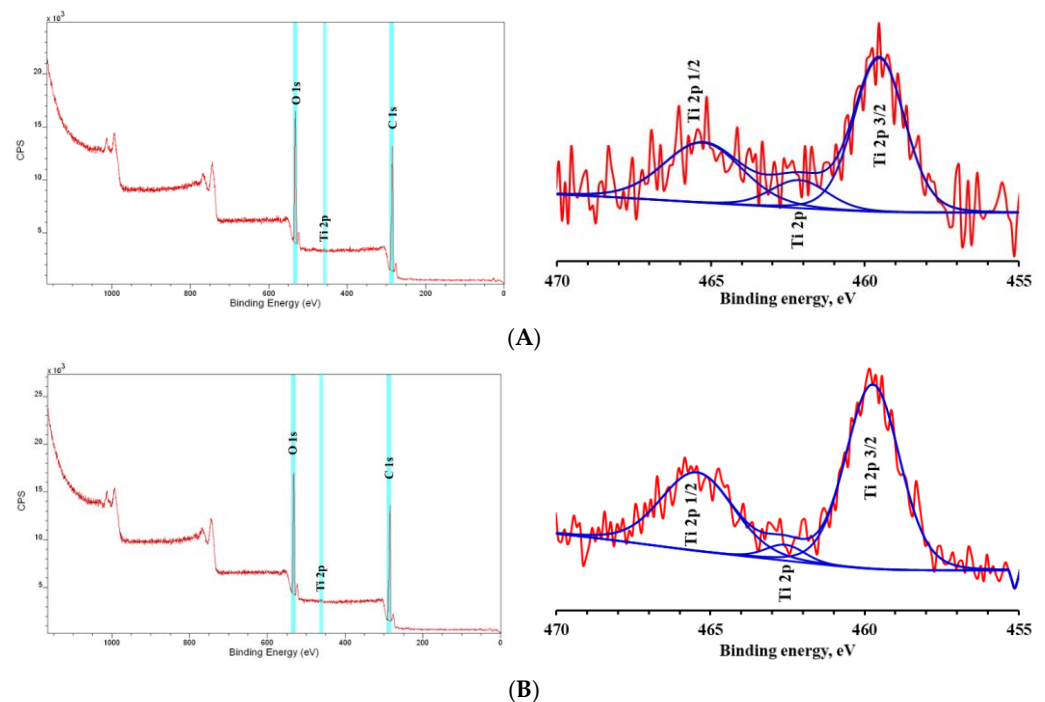


**Figure 2.** Survey XPS (left, bands for C1s, O1s, and Ti2p are marked in blue) and Ti2p (right, splitting is marked with blue lines) spectra of electrospun PMMA/5TiO<sub>2</sub> (A) and PMMA/10TiO<sub>2</sub> (B) composites.

The possibility of altering the surface wettability of the PMMA/TiO<sub>2</sub> composites was particularly crucial from a practical point of view. It is well known that UV light treatment enhances the wettability of different titanium surfaces [7,23]. SEM and XPS analyses unambiguously proved the presence of TiO<sub>2</sub> on the composites' surfaces. For that reason, the water contact angles were measured before and after UV light irradiation in order to study the alteration in surface wettability of the PMMA/TiO<sub>2</sub> composites. As seen in Figure 3, before UV irradiation the PMMA fibers showed water contact angles of  $111.5^\circ \pm 5.17^\circ$  due to their hydrophobic behavior [24]. As expected, the addition of TiO<sub>2</sub> led to the increase in contact angles to  $116.7^\circ \pm 3.75^\circ$  and  $122.6^\circ \pm 4.24^\circ$  for PMMA/5TiO<sub>2</sub> and PMMA/10TiO<sub>2</sub>, respectively. These results were in accordance with our previous findings and with the literature data [25,26]. Therefore, before UV irradiation the contact angles were in the hydrophobic region (above  $90^\circ$ ), which is due to the hydrophobic surface of the PMMA fibers. The presence of TiO<sub>2</sub> on the surfaces of the composites imparted additional hydrophobicity to the PMMA/TiO<sub>2</sub> composites. After 30 min of UV irradiation (Figure 3), the PMMA fibers remained hydrophobic and showed a water contact angle of  $112^\circ \pm 4.15^\circ$ . In contrast, the contact angles of PMMA/5TiO<sub>2</sub> and PMMA/10TiO<sub>2</sub> composites decreased significantly to  $93.5^\circ \pm 3.46^\circ$  and  $66.9^\circ \pm 2.36^\circ$ , respectively. It is noteworthy, however, that after 60 min of UV irradiation (Figure 3) only PMMA fibers preserved their hydrophobicity with a contact angle of  $109.8^\circ \pm 3.60^\circ$ , while the contact angle for both PMMA/5TiO<sub>2</sub> and PMMA/10TiO<sub>2</sub> was  $0^\circ$ . Thus, the change in the wettability of PMMA/TiO<sub>2</sub> composites strongly depends on the fiber surface composition, and a highly hydrophilic surface might be achieved by UV irradiation.

The crystal phase of  $\text{TiO}_2$  in the composite fibers was identified by X-ray diffraction (XRD) and compared with those of the PMMA fibers (Figure 4). The diffraction pattern of the PMMA fibers showed a broad diffraction plane at  $2\theta = 13.7^\circ$  (intensive), as well as at  $2\theta = 30.0^\circ$  and  $42.7^\circ$  (lower intensities), characteristic of its amorphous structure. In addition to these planes of PMMA, the XRD patterns of PMMA/ $\text{TiO}_2$  composites exhibited characteristic  $\text{TiO}_2$  diffraction peaks at  $2\theta = 25.6^\circ$  (101) and  $48.2^\circ$  (200) (Figure 4) for the anatase crystal phase. These results indicated that the  $\text{TiO}_2$  incorporated in the PMMA fibers did not affect the structure of PMMA and that these components did not react during the electrospinning. The obtained results are in agreement with the  $\text{TiO}_2$  (anatase) standard data (ICDD-PDF2 #00-021-1272).

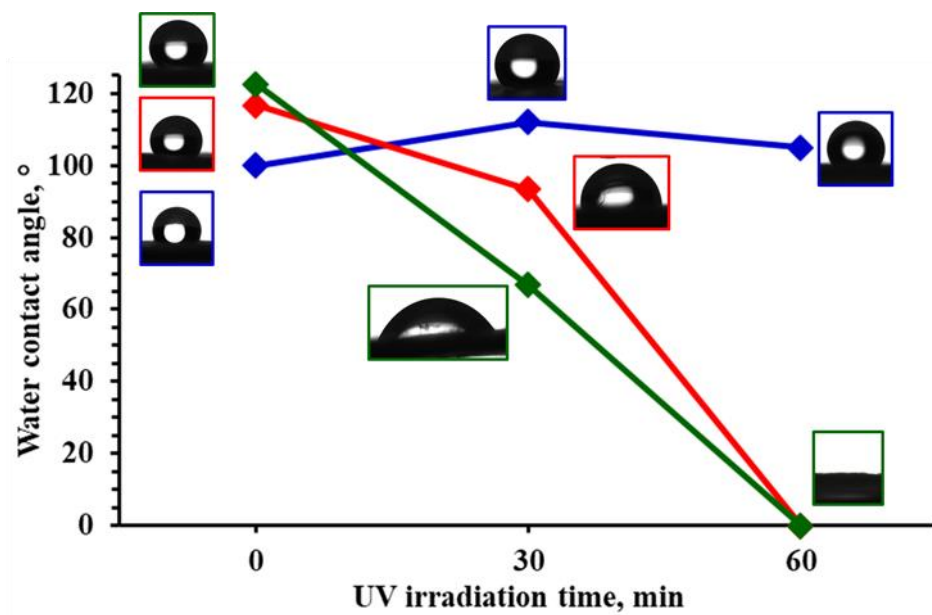


Figure 3. Water contact angles and digital images of water droplets on electrospun PMMA (blue), PMMA/5TiO<sub>2</sub> (red), and PMMA/10TiO<sub>2</sub> (green) composites before and after UV irradiation.

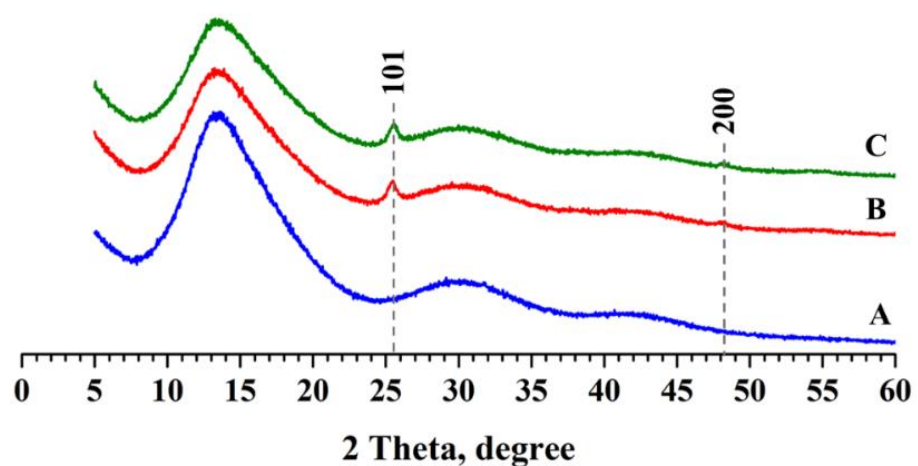


Figure 4. XRD patterns of electrospun PMMA (A), PMMA/5TiO<sub>2</sub> (B), and PMMA/10TiO<sub>2</sub> (C) composites.

The effect of  $\text{TiO}_2$  content on the thermal stability of the PMMA/ $\text{TiO}_2$  composites was studied by TGA (Figure 5). Apparently, the thermal decomposition of PMMA and composites began at 300 °C and ended at 400 °C due to the decomposition of PMMA. As can be seen, the thermal stability of the composites was slightly shifted to a higher decomposition temperature—373 °C for PMMA/5 $\text{TiO}_2$  and 375 °C for PMMA/10 $\text{TiO}_2$ —in comparison to that of PMMA fibers (369 °C). These results indicated that the addition of  $\text{TiO}_2$  slightly increased the thermal stability of the obtained composites. It is notable that in thermal decomposition of the PMMA/5 $\text{TiO}_2$  and PMMA/10 $\text{TiO}_2$  composites, the presence of 5.3% and 10.9% residues was observed (Figure 5, red and green lines). These residues are due to the inorganic  $\text{TiO}_2$  component, which did not undergo any alteration at these temperatures. These weight losses were very close to the initial  $\text{TiO}_2$  amounts added to the PMMA solutions.

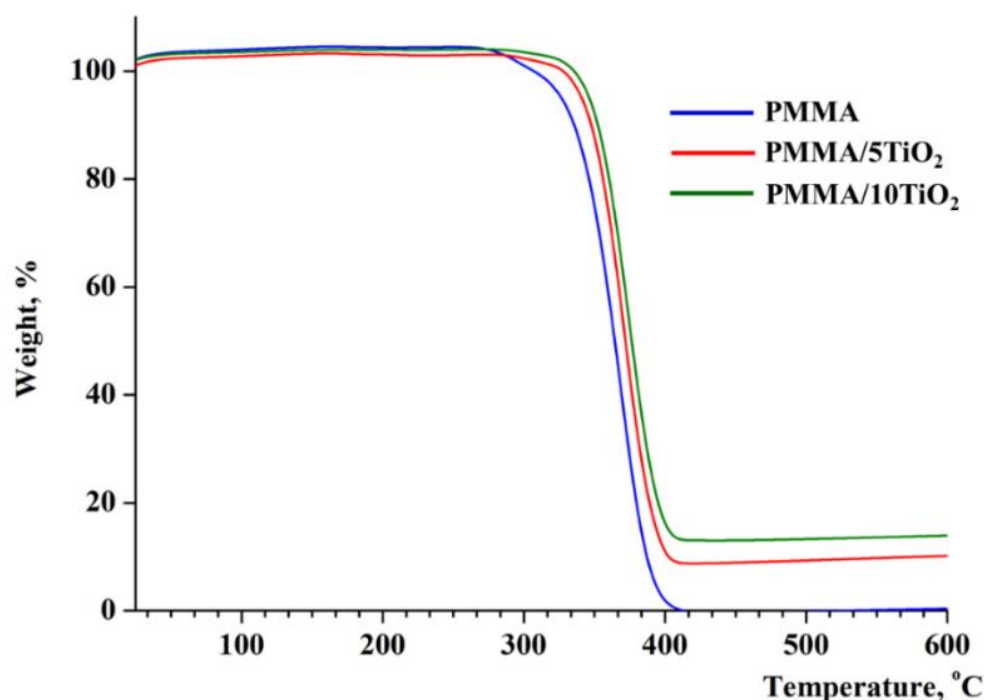
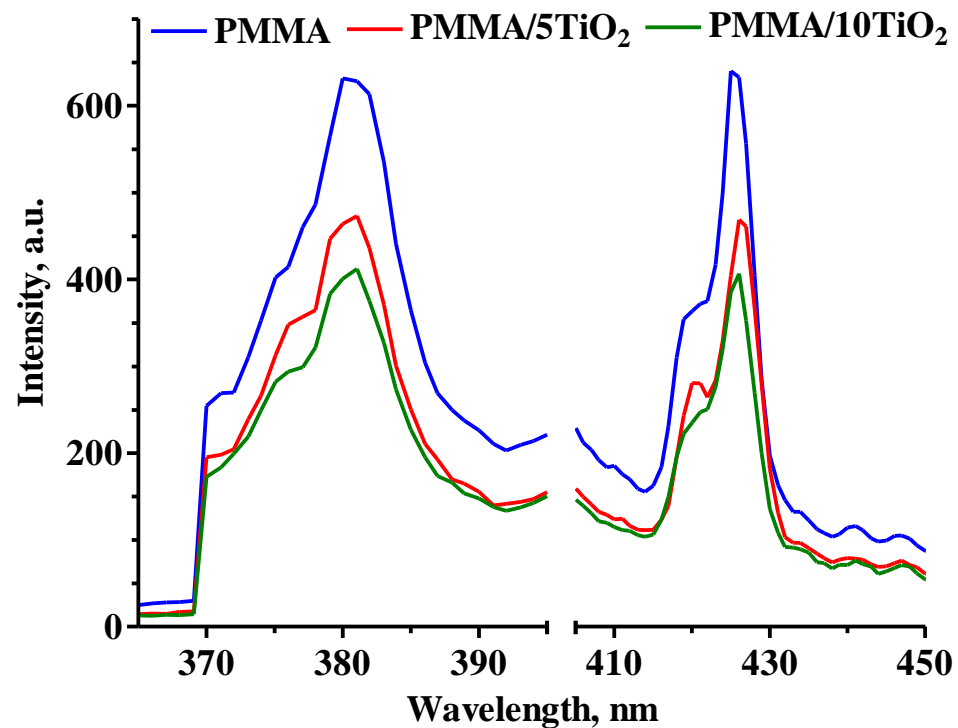


Figure 5. TG curves of electrospun PMMA, PMMA/5 $\text{TiO}_2$ , and PMMA/10 $\text{TiO}_2$  composites.

In order to study the effect of the  $\text{TiO}_2$  content on the optical properties of PMMA, the excitation and emission spectra of electrospun materials were recorded and compared (Figure 6). The excitation spectrum of PMMA fibers had a maximum at 380 nm, which corresponds to the absorption maximum of the polymer, while its fluorescence maximum was at 425 nm. Interestingly, the fluorescence intensity was quenched upon the addition of  $\text{TiO}_2$ , and this quenching depended on the amount of  $\text{TiO}_2$  added. The same positions of the maxima in the spectra indicate that  $\text{TiO}_2$  did not change the structure of the PMMA matrix. On the other hand, the decrease in the fluorescence intensity can be explained by the interaction of  $\text{TiO}_2$  with the lone pairs of oxygen atoms in the structure of PMMA, which led to a change in its polarization.





**Figure 6.** Excitation spectra (left) and the corresponding emission spectra (right) of electrospun PMMA (blue line), PMMA/5TiO<sub>2</sub> (red line), and PMMA/10TiO<sub>2</sub> (green line) membranes.

### 3.2. Tensile Properties of the PMMA/TiO<sub>2</sub> Composites

In view of the potential application of these composites, we decided to study their tensile strength and compare the values obtained with those of PMMA. A serious problem in the accurate evaluation of the mechanical properties of electrospun materials is the lack of standardization in conducting tensile tests. Recently, we showed that specimens cut in the direction of the collector rotation (0°) have better mechanical properties [27]. For that reason, this already developed standardized methodology was applied for the tensile testing of the electrospun composites. The average thickness of all specimens was ~0.312 mm.

Stress–strain ( $\sigma/\varepsilon$ ) curves performed at tension of specimens at a constant rate are shown in Figure 7. All curves showed a smooth linear increase in the stress with increasing strain. The curve for PMMA fibers displayed a high deformation at relatively low stress. As can be seen, the composite fibers had better mechanical properties compared to the PMMA fibers. Moreover, the addition of TiO<sub>2</sub> resulted in a proportional increase in the stress with increasing strain, which ended with the sample breaking.

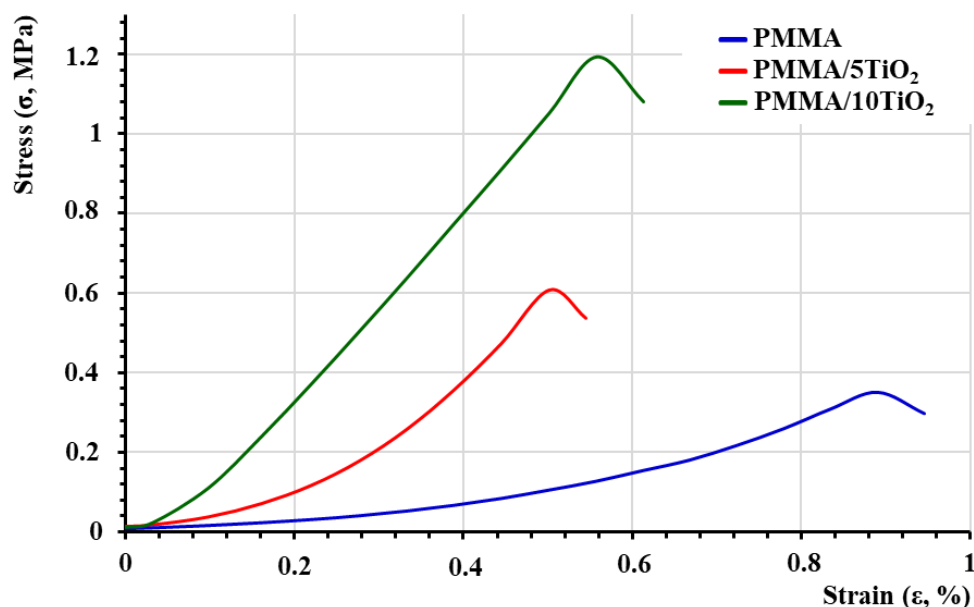


**Figure 7.** Stress–strain curves of electrospun PMMA (blue line), PMMA/5TiO<sub>2</sub> (red line), and PMMA/10TiO<sub>2</sub> (green line) composites.

From the stress–strain curves, the values of the modulus of elasticity ( $E$ , MPa), tensile strength ( $\sigma$ , MPa), and elongation at break ( $\epsilon_B$ , %) were determined; these are presented in Table 1. It is obvious that the composite materials had a higher modulus of elasticity and tensile strength compared to the PMMA fibers. Furthermore, the tensile strength of the composites increased almost twice as the TiO<sub>2</sub> amount increasing. In contrary, the elongation at break of the PMMA fibers was more than three times greater than that of the composites. These results indicate that the addition of TiO<sub>2</sub> improved the elasticity of the composites and contributed to reducing their brittleness. In addition, the composites provided a higher loading.

**Table 1.** The mechanical characteristics of electrospun materials.

Samples	Young's Modulus ( $E$ , MPa)	Tensile Strength ( $\sigma$ , MPa)	Elongation at Break ( $\epsilon_B$ , %)
PMMA	82.4	0.50	1.95
PMMA/5TiO <sub>2</sub>	237.4	0.61	0.50
PMMA/10TiO <sub>2</sub>	251.9	1.19	0.56

### 3.3. Photocatalytic Degradation of MB and Reusability of PMMA/TiO<sub>2</sub> Composites

The photocatalytic activity of the composites was studied in the presence of the model organic pollutant—methylene blue (MB)—and monitored spectrophotometrically at 660 nm. The obtained results show a decrease in MB absorption as a function of irradiation time (Figure 8). It can be seen that PMMA/5TiO<sub>2</sub> composites degrade ca. 20% of the dye after 30 min of irradiation, while after 60 min they degrade approximately 50%. Clearly, in the presence of PMMA/10TiO<sub>2</sub> composites, 50% of the dye degraded after 30 min—i.e., composites containing large amounts of TiO<sub>2</sub> were more effective. This effect was expected, because the amount of TiO<sub>2</sub> particles is higher on the surface of PMMA/10TiO<sub>2</sub> composites, which accelerates the photocatalytic action.

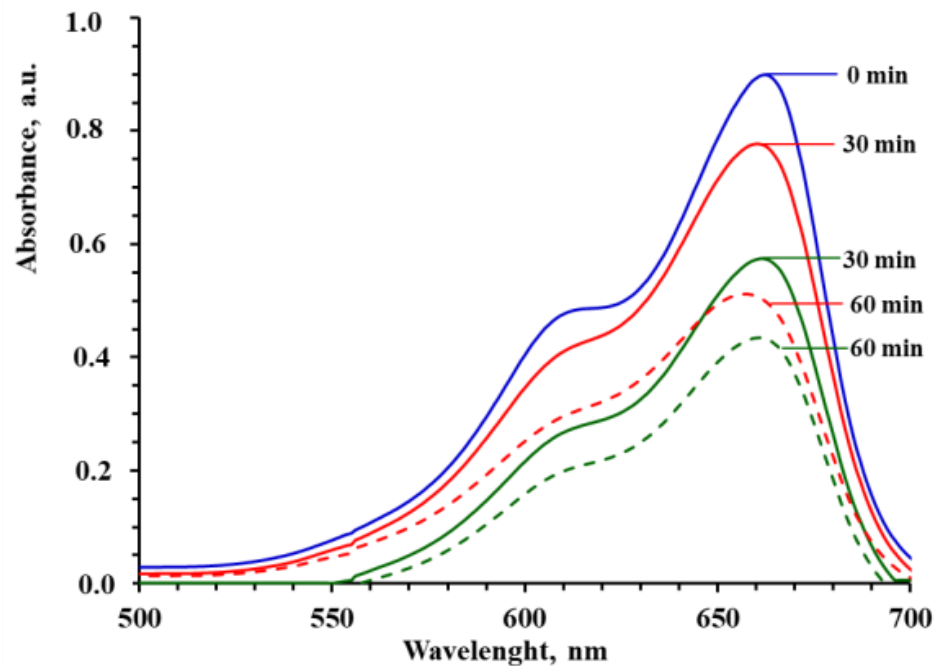
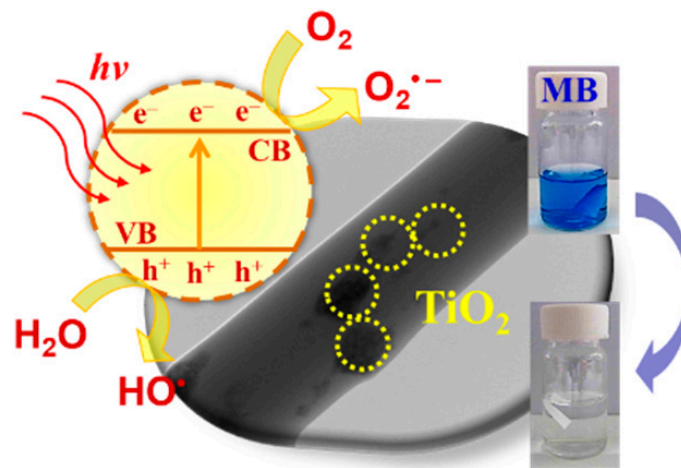


**Figure 8.** Absorption spectra of MB (blue line) after UV light irradiation (30 and 60 min) in the presence of electrospun PMMA/5TiO<sub>2</sub> (red lines) and PMMA/10TiO<sub>2</sub> (green lines) composites.

Schematic representation of the photocatalytic degradation of MB in the presence of PMMA/TiO<sub>2</sub> composites is shown in Scheme 1.



**Scheme 1.** Representation of the photocatalytic degradation of MB in the presence of PMMA/TiO<sub>2</sub> composites.

The photocatalytic activity of the composites during three irradiation cycles was also measured in order to evaluate their activity during repeated use (Figure 9). The reaction of a blank sample (PMMA fibers) was monitored as well. As can be seen, in the presence of PMMA fibers, MB preserved its stability and a very slight discoloration under UV irradiation was observed (Figure 9, blue line). After 9 h of irradiation, the calculated photodegradation efficiency was only 11.5%. Thus, the photocatalytic activity of the composites was determined to be due to the embedded TiO<sub>2</sub>. Undoubtedly, the composites exhibited excellent stability—at the end of the third cycle, the calculated PDEs were 95.8% and 99.1% in the presence of PMMA/5TiO<sub>2</sub> and PMMA/10TiO<sub>2</sub>, respectively. These results prove that the composites maintain their photocatalytic activity even after three uses.

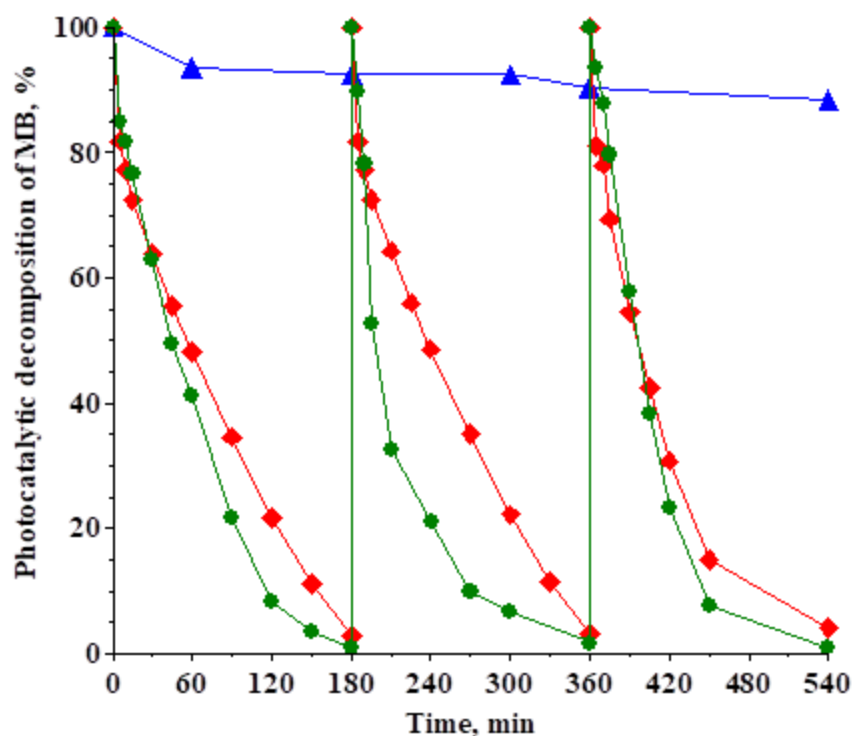


**Figure 9.** Three consecutive cycles of MB degradation at 660 nm under UV light irradiation in the presence of electrospun PMMA (blue line), PMMA/5TiO<sub>2</sub> (red line), and PMMA/10TiO<sub>2</sub> (green line) composites.

#### 4. Conclusions

In the present study, PMMA/TiO<sub>2</sub> composites were successfully fabricated in one step by electrospinning. Besides the electrospinning conditions, the TiO<sub>2</sub> content in the PMMA solution was varied in order to fabricate PMMA fibers filled with significant amounts of TiO<sub>2</sub>. It was shown that the incorporation of a maximum of 10% TiO<sub>2</sub> into the PMMA solution did not hamper the electrospinning and resulted in the preparation of continuous and defect-free composite fibers. Clearly, the morphology and surface chemical composition of electrospun PMMA/TiO<sub>2</sub> fibers depends on the TiO<sub>2</sub> content. Contact angle measurements revealed that the wettability of the composites might be easily changed from hydrophobic to superhydrophilic after 1 h of UV light irradiation. In particular, TiO<sub>2</sub> had a slight impact on the thermal stability and optical properties of the composites. However, the incorporation of the inorganic component resulted in a significant increase in the modulus of elasticity and tensile strength and a decrease in elongation at break. Furthermore, PMMA/TiO<sub>2</sub> composites preserve their photocatalytic activity almost completely after three uses in the presence of a model organic pollutant. Thus, the proposed original and simple approach is very promising for the future development of highly efficient membranes for the degradation of organic pollutants.

**Supplementary Materials:** The following are available online at <https://www.mdpi.com/article/10.3390/polym13223923/s1>, Figure S1: TEM micrograph and SAED patterns of the PMMA/5TiO<sub>2</sub> composites.

**Author Contributions:** Conceptualization, O.S. and I.R.; methodology O.S. and I.R.; investigation, O.S.; writing—original draft preparation, O.S.; writing—review and editing, I.R. and N.M.; visualization, O.S. and I.R.; project administration, O.S. All authors have read and agreed to the published version of the manuscript.

**Funding:** Research equipment of Distributed Research Infrastructure INFRAMAT, part of Bulgarian National Roadmap for Research Infrastructures, supported by Bulgarian Ministry of Education and Science was used in this investigation.

**Institutional Review Board Statement:** Not applicable.

**Informed Consent Statement:** Not applicable.

**Data Availability Statement:** The data presented in this study are available on request from the corresponding author.

**Acknowledgments:** Research equipment of Distributed Research Infrastructure INFRAMAT, part of the Bulgarian National Roadmap for Research Infrastructures, supported by the Bulgarian Ministry of Education and Science, was used in this study. This research was partially funded by the European Regional Development Fund within the Operational Programme “Science and Education for Smart Growth 2014–2020”, grant number BG05M2OP001-1.001-0008-C01.

**Conflicts of Interest:** The authors declare no conflict of interest.

## References

1. Liao, Y.; Loh, C.-H.; Tian, M.; Wang, R.; Fane, A.G. Progress in electrospun polymeric nanofibrous membranes for water treatment: Fabrication, modification and applications. *Prog. Polym. Sci.* **2018**, *77*, 69–94. [[CrossRef](#)]
2. Asmatulu, R.; Khan, W.S. Chapter 7—Electrospun nanofibers for filtration applications. In *Synthesis and Applications of Electrospun Nanofibers (Micro and Nano Technologies)*, 1st ed.; Asmatulu, R., Khan, W.S., Eds.; Elsevier Inc.: Amsterdam, The Netherlands, 2019; pp. 135–152.
3. Ray, S.S.; Chen, S.-S.; Nguyen, N.C.; Nguyen, H.T. Chapter 9—Electrospinning: A Versatile Fabrication Technique for Nanofibrous Membranes for Use in Desalination. In *Nanoscale Materials in Water Purification (Micro and Nano Technologies)*; Thomas, S., Pasquini, D., Leu, S.-Y., Gopakumar, D.A., Eds.; Elsevier Inc.: Amsterdam, The Netherlands, 2019; pp. 247–273.
4. El Nazer, H.E.A.F.A.H.; Gaballah, S.T. Nanocomposites and Its Importance in Photocatalysis. In *Nanocomposites for Visible Light-Induced Photocatalysis*; Khan, M., Pradhan, D., Sohn, Y., Eds.; Springer Series on Polymer and Composite Materials; Springer: Berlin/Heidelberg, Germany, 2017; pp. 41–67.
5. Pirilä, M.; Saouabe, M.; Ojala, S.; Rathnayake, B.; Drault, F.; Valtanen, A.; Huuhtanen, M.; Brahmi, R.; Keiski, R.L. Photocatalytic degradation of organic pollutants in wastewater. *Top. Catal.* **2015**, *58*, 1085–1099. [[CrossRef](#)]
6. Rajeshwar, K.; Osugi, M.E.; Chanmanee, W.; Chenthamaraksha, C.R.; Zaroni, M.V.B.; Kajitvichyanukul, P.; Krishnan-Ayer, R. Heterogeneous photocatalytic treatment of organic dyes in air and aqueous media. *J. Photochem. Photobiol. C Photochem. Rev.* **2008**, *9*, 171–192. [[CrossRef](#)]
7. Nakata, K.; Fujishima, A. TiO<sub>2</sub> photocatalysis: Design and applications. *J. Photochem. Photobiol. C Photochem. Rev.* **2008**, *13*, 169–189. [[CrossRef](#)]
8. Linsebigler, A.L.; Lu, G.; Yates, J.T. Photocatalysis on TiO<sub>2</sub> surfaces: Principles, mechanisms, and selected results. *Chem. Rev.* **1995**, *95*, 735–758. [[CrossRef](#)]
9. Dahl, M.; Liu, Y.; Yin, Y. Composite titanium dioxide nanomaterials. *Chem. Rev.* **2014**, *114*, 9853–9889. [[CrossRef](#)]
10. Ali, U.; Abd Karim, K.J.B.; Buang, N.A. A review of the properties and applications of poly (methyl methacrylate) (PMMA). *Polym. Rev.* **2015**, *55*, 678–705. [[CrossRef](#)]
11. Cantarella, M.; Sanz, R.; Buccheri, M.A.; Ruffino, F.; Rappazzo, G.; Scalese, S.; Impellizzeri, G.; Romano, L.; Privitera, V. Immobilization of nanomaterials in PMMA composites for photocatalytic removal of dyes, phenols and bacteria from water. *J. Photochem. Photobiol. A Chem.* **2016**, *321*, 1–11. [[CrossRef](#)]
12. Sengwa, R.J.; Dhatarwal, P. Polymer nanocomposites comprising PMMA matrix and ZnO, SnO<sub>2</sub>, and TiO<sub>2</sub> nanofillers: A comparative study of structural, optical, and dielectric properties for multifunctional technological applications. *Opt. Mater.* **2021**, *113*, 110837–110848. [[CrossRef](#)]
13. Nandimath, M.; Bhajantri, R.F.; Naik, J.; Hebbar, V. Effect of Rhodamine 6G dye on chromaticity co-ordinates and photoluminescence properties of TiO<sub>2</sub>/PMMA polymer nanocomposites for LED applications. *J. Lumin.* **2019**, *207*, 571–584. [[CrossRef](#)]
14. Li, C.; Yu, H.; Song, Y.; Liang, H.; Yan, H. Preparation and characterization of PMMA/TiO<sub>2</sub> hybrid shell microencapsulated PCMs for thermal energy storage. *Energy* **2019**, *167*, 1031–1039. [[CrossRef](#)]
15. Cantarella, M.; Sanz, R.; Buccheri, M.A.; Romano, L.; Privitera, V. PMMA/TiO<sub>2</sub> nanotubes composites for photocatalytic removal of organic compounds and bacteria from water. *Mater. Sci. Semicond. Process.* **2016**, *42*, 58–61. [[CrossRef](#)]
16. Zhao, J.; Yang, Y.; Li, Y.; Zhao, L.; Wang, H.; Song, G.; Tang, G. Microencapsulated phase change materials with TiO<sub>2</sub>-doped PMMA shell for thermal energy storage and UV-shielding. *Sol. Energy Mater. Sol. Cells* **2017**, *168*, 62–68. [[CrossRef](#)]
17. Sugumaran, S.; Bellan, C. Transparent nano composite PVA–TiO<sub>2</sub> and PMMA–TiO<sub>2</sub> thin films: Optical and dielectric properties. *Optik* **2014**, *125*, 5128–5133. [[CrossRef](#)]
18. Koysuren, O.; Koysuren, H.N. Photocatalytic activities of poly(methyl methacrylate)/titanium dioxide nanofiber mat. *J. Macromol. Sci. Part A Pure Appl. Chem.* **2017**, *54*, 80–84. [[CrossRef](#)]
19. Korina, E.; Stoilova, O.; Manolova, N.; Rashkov, I. Multifunctional hybrid materials from poly(3-hydroxybutyrate), TiO<sub>2</sub> nanoparticles, and chitosan oligomers by combining electrospinning/electrospraying and impregnation. *Macromol. Biosci.* **2013**, *13*, 707–716. [[CrossRef](#)]

20. Korina, E.; Stoilova, O.; Manolova, N.; Rashkov, I. Poly(3-hydroxybutyrate)-based hybrid materials with photocatalytic and magnetic properties prepared by electrospinning and electrospaying. *J. Mater. Sci.* **2014**, *49*, 2144–2153. [[CrossRef](#)]
21. Korina, E.; Stoilova, O.; Manolova, N.; Rashkov, I. Polymer fibers with magnetic core decorated with titanium dioxide prospective for photocatalytic water treatment. *J. Environ. Chem. Eng.* **2018**, *6*, 2075–2084. [[CrossRef](#)]
22. Casaletto, M.P.; Ingo, G.M.; Kaciulis, S.; Mattogno, G.; Pandol, L.; Scavia, G. Surface studies of in vitro biocompatibility of titanium oxide coatings. *Appl. Surf. Sci.* **2001**, *172*, 167–177. [[CrossRef](#)]
23. Wang, R.; Hashimoto, K.; Fujishima, A.; Chikuni, M.; Kojima, E.; Kitamura, A.; Shimohigoshi, M.; Watanabe, T. Light-induced amphiphilic surfaces. *Nature* **1997**, *388*, 431–432. [[CrossRef](#)]
24. Ma, M.; Gupta, M.; Li, Z.; Zhai, L.; Gleason, K.K.; Cohen, R.E.; Rubner, M.F.; Rutledge, G.C. Decorated electrospun fibers exhibiting superhydrophobicity. *Adv. Mater.* **2007**, *19*, 255–259. [[CrossRef](#)]
25. Spasova, M.; Stoilova, O.; Manolova, N.; Rashkov, I.; Naydenov, M. Electrospun eco-friendly materials based on poly(3-hydroxybutyrate) and TiO<sub>2</sub> with antifungal activity prospective for Esca treatment. *Polymers* **2020**, *12*, 1384–1395. [[CrossRef](#)] [[PubMed](#)]
26. Nowak, E.; Combes, G.; Hugh Stitt, E.; Pacek, A.W. A comparison of contact angle measurement techniques applied to highly porous catalyst supports. *Powder Technol.* **2013**, *233*, 52–64. [[CrossRef](#)]
27. Borisova, I.; Stoilova, O.; Manolova, N.; Rashkov, I. Effect of coating on the mechanical properties of electrospun poly(3-hydroxybutyrate) materials with targeted fibers alignment. *J. Polym. Res.* **2021**, *28*, 1–13. [[CrossRef](#)]